Journal of Cardiovascular Magnetic Resonance®, 4(1), 170–180 (2002)

Poster Abstracts: Clinical MRI— Non-Ischemic Acquired HD

314. Gender Differences in Detection of Concentric Left Ventricular Geometry by Magnetic Resonance Imaging

Michael Chuang,[1] Carol Salton,[2] Christopher O'donnell,[3] Kraig Kissinger,[1] Daniel Levy,[3] Warren Manning.[1] [1]*Beth Israel Deaconess Medical Center, Cardiovascular Division, Boston, Massachusetts, United States;* [2]*Beth Israel Deaconess Medical Center, 330 Brookline Avenue, Boston, MA, United States;* [3]*NHLBI's Framingham Heart Study, 5 Thurber Street, Framingham, Massachusetts, United States*

Introduction: Left ventricular (LV) concentric geometry (CONC), defined echocardiographically as a basal septal wall thickness to LV cavity radius ratio (WTCR) ≥ 0.45, is associated with excess cardiovascular risk. Given the accuracy and reproducibility advantages of volumetric imaging, criteria for CONC based on volumetric measures are desirable.

Purpose: We prospectively selected LV mass divided by end-diastolic volume (EDV), a mass-to-volume ratio, or MVR, as a volumetric analog to the linear WTCR and sought to compare these two indexes for stratification of a population-based sample for CONC.

Methods: Subjects: 292 (141 men, 151 women) adult members of the Framingham Heart Study Offspring Cohort who were free of symptomatic cardiovascular disease were studied. The mean ± SD age of the subjects was 59 ± 9 years. All subjects provided written informed consent.

Image Acquisition and Analysis: MRI used a 1.5-T Gyroscan ACS/NT (Philips Medical Systems, Best, NL), cardiac array coil and a TFE-EPI breathhold cine sequence. Eight to ten 10-mm thick contiguous LV short-axis slices were used to encompass the left ventricle during end-tidal breath-holds. Image analysis was performed on an EasyScil workstation (Philips) by a single expert observer. For volumetric analysis, endocardial and epicardial borders were manually segmented from end-diastolic images and volumes were computed using a summation of disks method. LV mass was computed as the difference between end-diastolic epicardial and endocardial volumes multiplied by 1.05 g/ml. Linear measurements were obtained from a basal end-diastolic slice at the level of the chordae for interventricular septal wall thickness (IVS) and for end-diastolic dimension (EDD).

Data Analysis: MVR was computed as LV mass/EDV and WTCR as 2*IVS/EDD. Three subanalyses were performed. First, defining WTCR measures as "truth," subjects with WCR ≥ 0.45 were classified as having CONC. We then used ROC analysis to identify gender-specific optimal thresholds for MVR for identification of CONC by volumetric measures. Second, we stratified subjects into quartiles of CONC based on WTCR and again, separately, based on MVR. The number and type of interquartile crossovers between WCR and MVR were tabulated. Finally, we ranked subjects using MVR and WTCR and computed Pearson correlation to assess the relationships between the two measures for men and for women.

Results: ROC analysis indicated that an overall MVR threshold of 1.45 was optimal for identification of CONC, with SENS = 53% and SPEC = 73% when considering all 292 subjects. Gender-specific analyses indicated MVR ≥ 1.40 gave SENS = 72%, SPEC = 73% for the 151 women, while MVR ≥ 1.45 yielded SENS = 58%, SPEC = 65% for the 141 men. Stratification of all subjects by quartiles of CONC revealed similar agreement between WTCR and MVR for

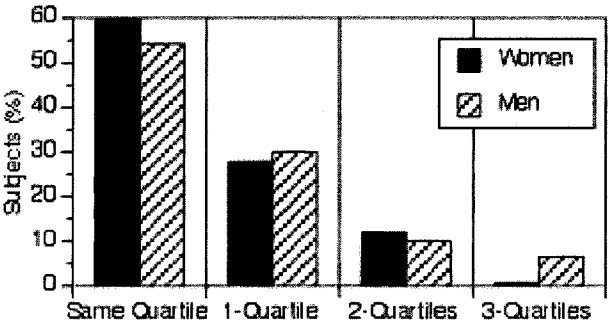

Figure 1.

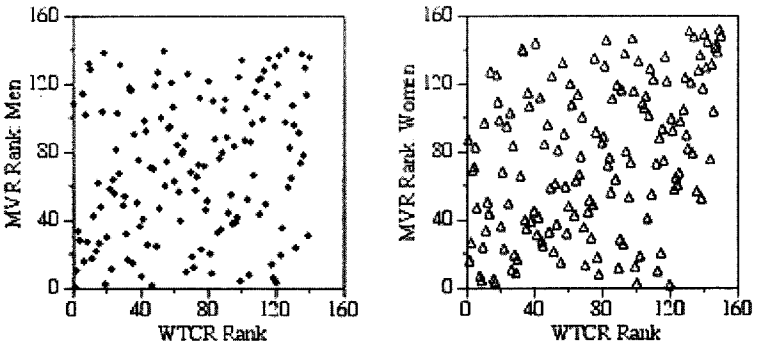

Figure 2.

women and men (Figure 1). For each gender slightly over half of subjects were assigned to the same quartile of CONC by WTCR and MVR. The proportion of subjects with 1-, 2- and 3-quartile differences declined monotonically as seen in Figure 1. There were no differences in distribution of interquartile differences regardless of CONC status; the agreement between WTCR and MVR was neither better nor worse in the presence of concentric LV geometry. Finally, there was weak but statistically significant correlation between WTCR and MVR for women ($r = 0.56$, $p < 0.001$) and for men ($r = 0.25$, $p < 0.005$). When subjects were assigned gender-specific numerical ranks with respect to degree of CONC, there was again statistically significant correlation (women: $r = 0.40$, $p < 0.005$, men: $r = 0.21$, $p < 0.02$) but substantial individual variation in ranking by WTCR and MVR, as shown in Figure 2.

Conclusion: The agreement between current linear measurement-based criteria for CONC and MVR is only modest with respect to stratification of patients by CONC. Use of gender-specific thresholds for CONC indicates greater agreement between linear and volumetric criteria for women than men, but there remains substantial individual variation between WTCR-based and MVR-based assessment of CONC. Volumetric assessment of the LV has many advantages over linear measures, including greater reproducibility and lack of dependence of geometric models of LV shape. However, there is no widely accepted definition of CONC based on volumetric measures. We selected one possible and "natural" volumetric index of CONC, the end-diastolic mass to volume ratio, MVR, and have shown that it cannot be used interchangeably with the WTCR, as there is substantial variation between the two measures when applied to individual subjects. Further work is needed to determine whether MVR, or some other volumetric measure, is a useful index of CONC, and whether gender-specific thresholds can improve the prognostic value.

315. Myocardial and Respiratory Muscle Abnormalities in Patients with Duchenne Muscular Dystrophy: An MRI Study

Sophie Mavrogeni,[1] George Tzelepis,[1] George Athanasopoulos,[1] Themistoklis Maounis,[1] Genovefa Kolovou,[1] Marouso Douskou,[2] Sotirios Giouroukos,[3] Aikaterini Papavasiliou,[4] Dennis Cokkinos.[1] [1]*Onassis Cardiac Surgery Center, 50 Esperou Street, P.Faliro, Athens, Greece;* [2]*Bioiatriki MRI Unit, Athens, Greece;* [3]*Aghia Sophia Childrens' Hospital, Athens, Greece;* [4]*Pentelis Childrens' Hospital, Athens, Greece*

Introduction: Myocardial and respiratory muscle dysfunction is a significant cause of morbidity and mortality in patients with Duchenne Muscular Dystrophy (DMD).

Purpose: In a group of patients with DMD and no clinical evidence of respiratory or cardiac involvement, we applied Magnetic Resonance Imaging (MRI) to characterize the status of the myocardial and respiratory muscle tissue.

Methods: Twelve male patients aged 19 (17–20) years and 10 age-matched controls were included in the study. All patients had a normal Echocardiographic, Holter and spirometric examination. MRI was performed with a 0.5 T machine. A coronal spin-echo plane was used for sternocleidomastoid (SCM) muscle localization and a horizontal long-axis spin-echo plane for left ventricular study. Myocardial and right (R) and left (L) SCM muscle T2 relaxation time was calculated using 4 TEs (17–68 msec) and TR = heart rate.

Results: In comparison to controls, patients with DMD had lower T2 relaxation time of the heart (T2 H: 35 ± 5 vs. 63 ± 3 msec, $p < 0.001$) and lower T2 relaxation time of right and left SCM muscle (T2 SCM-R: 26 ± 3 vs. 42 ± 1 msec, $p < 0.001$ and T2 SCM-L: 23 ± 3 vs. 42 ± 2 msec, $p < 0.001$). In patients with DMD, the T2 relaxation time of the heart did not correlate with that of the SCM ($r = 0.016$, $p =$ NS).

Conclusion: In conclusion, the MRI can detect abnormalities in both the myocardium and the respiratory muscles in patients with Duchenne Muscular Dystrophy, who have no clinical evidence of respiratory or cardiac dysfunction. The MRI is a non-invasive, easily reproducible diagnostic modality that can be used to assess muscle status and possibly monitor disease progression in patients with DMD.

316. MRI Perfusion Patterns in Hypertrophic Cardiomyopathy Patients Undergoing Non-surgical Septal Reduction Therapy

Katherine Wu,[1] Alan Heldman,[1] Jeffrey Brinker,[1] Joshua Hare,[1] Joao Lima.[1] [1]*Johns Hopkins University, Carnegie 568, Baltimore, Maryland, United States*

Introduction: Patients with hypertrophic cardiomyopathy may develop incapacitating symptoms because of left ventricular outflow tract (LVOT) obstruction. Therapeutic strategies aimed at reducing the LVOT gradient include medications, pacing, and surgical myotomy/myectomy to resect the proximal ventricular septum. Recently, a less invasive technique, termed non-surgical septal reduction therapy (NSSRT) (1) has been developed. This involves angiographic delineation of the proximal septal branch(es) of the left anterior descending artery. The septal artery is then injected with ethanol through an occlusive balloon to create a localized infarct. This leads to regression and thinning of the proximal ventricular septum, thus reducing the LVOT gradient. Myocardial perfusion and microvascular function affect prognosis and left ventricular remodeling after acute myocardial infarction (MI) (2,3). The mechanism of infarction and prognostic implications of NSSRT are not well-understood.

Purpose: To use contrast-enhanced MRI to describe myocardial perfusion patterns seen after NSSRT.

Methods: We performed contrast-enhanced MRI with a 1.5 T magnet (Signa, GE) at baseline, pre-NSSRT, and within 4 days post-NSSRT in 3 patients. Gadolinium 0.2 mmol/kg was bolus injected intravenously. Short-axis first-pass images were obtained using a gradient-echo echo-planar sequence (efgret): matrix 128 × 128, FOV = 36, TR = 6.3, TE = 1.6, ETL = 4, image temporal resolution = 120 msec. Short and long-axis delayed images (10 minutes post-contrast) were obtained using an inversion-recovery gradient-echo sequence: matrix 256 × 160, TI = 200, flip angle = 20.

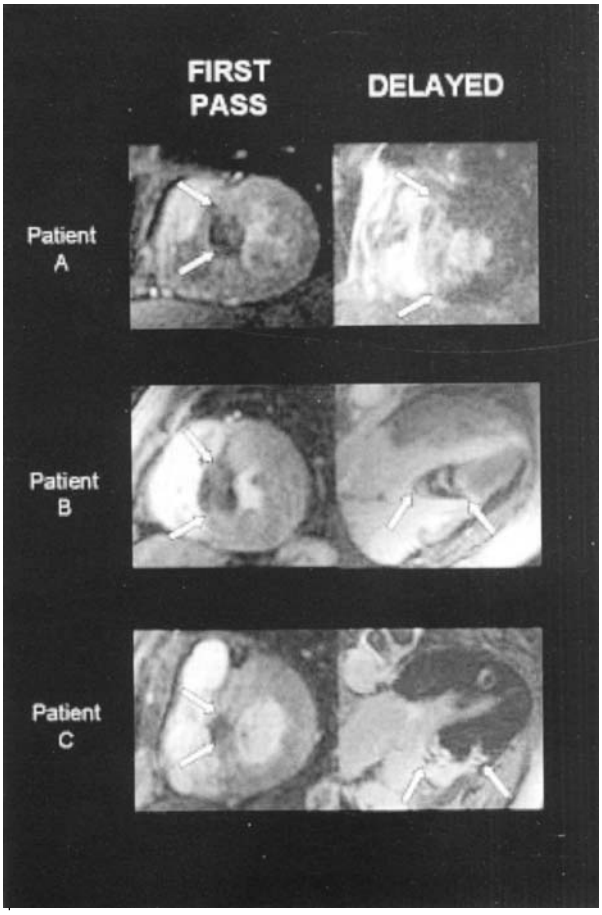

Figure 1.

Results: Baseline MR images in all 3 patients show marked left ventricular hypertrophy with homogeneous perfusion of the ventricular septum. One to three septal arteries per patient were treated with ethanol. Final angiography revealed slow or absent flow into the septal arteries. Post-NSSRT, first pass images (see Figure) show a striking transmural region of hypoenhancement or perfusion defect in all 3 patients. On the delayed images (see Figure), the pattern of hyperenhancement is much more variable. Patient A has a transmural region of hyperenhancement; patient B has patchy hyperenhancement with persistent hypoenhancement; and Patient C has 2 wedge-shaped regions correlating with the 2 treated septal branches.

Conclusion: The mechanism by which NSSRT leads to myocardial infarction appears to be dominated by microvessel occlusion with evidence of profound first-pass hypoenhancement by MRI. This differs from the MRI pattern that has been described following acute MI (2,4). Acute MI also results in a region of first pass hypoenhancement and an area of hyperenhancement on delayed imaging. However, the distribution and pattern of perfusion abnormalities are different in NSSRT. Whereas in acute MI, the hypoenhanced region is subendocardial (2,3,4), NSSRT causes transmural hypoenhancement. In contrast, the pattern of delayed hyperenhancement is transmural and homogeneously bright after acute MI while it is much more heterogeneous and patchy post-NSSRT. NSSRT thus represents a unique form of myocardial infarction in which the pathophysiologic mechanism may be that of severe microvascular damage. In patients with acute MI, the presence of microvascular obstruction predicts poor long-term outcome (2) and leads to worse ventricular remodeling (3). The long-term effects of NSSRT on hypertrophic cardiomyopathy patients remain unknown.

317. Interscanner Reproducibility of T2* Measurements for the Assessment of Tissue Iron Concentration

Mark Westwood,[1] Lisa Anderson,[2] Christine Lorenz,[3] Dudley Pennell.[4] [1]*Royal Brompton Hospital, Sydney Street, London, UK;* [2]*National Health Service, Sydney Street, London, United Kingdom;* [3]*Washington University in St. Louis, CMR Unit, London, United Kingdom;* [4]*Royal Brompton and Harefield NHS Trust, Sydney Street, London, United Kingdom*

Introduction: Heart failure caused by myocardial iron overload is the commonest cause of death in thalassemia major, and once symptoms develop, the outlook is poor. A magnetic resonance, gradient echo technique for quantifying tissue iron by using T2* measurements, has been previously validated against tissue iron concentrations. We now demonstrate that this technique is reproducible between MRI scanners.

Purpose: The aim of this study was to demonstrate that the assessment of tissue iron concentration using T2* relaxometry was reproducbile between MRI scanners.

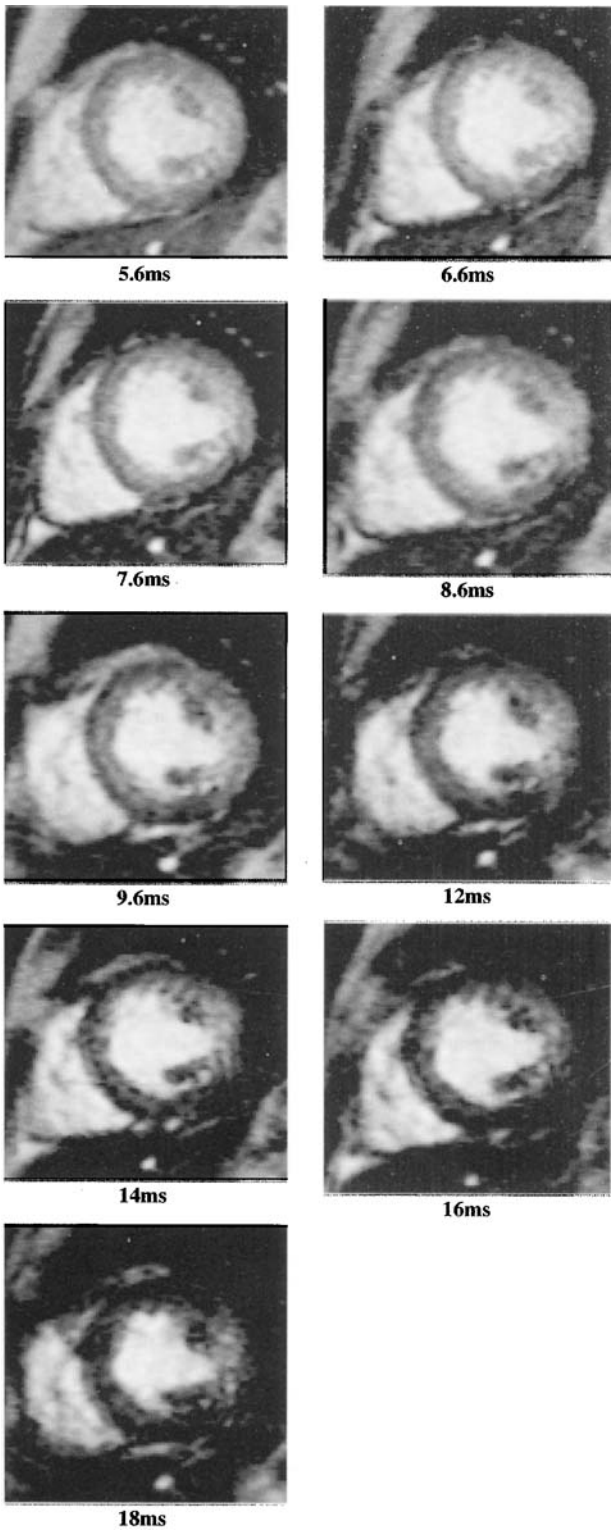

Figure 1. Method of calculation of $T2^*$ for the myocardium.

Methods: 25 patients with thalassaemia major requiring regular blood transfusions were selected for liver and heart iron assessment using a method previously described by Anderson et al[1] using a Picker 1.5T Edge Scanner (Marconi Medical Systems, Cleveland, Ohio). For the measurement of myocardial $T2^*$, a single short axis mid-ventricular slice was acquired at nine separate echo times (5.6–17.6 ms) and the repetition time between two radio-frequency pulses was between 11.81 and 23.81 ms, depending on the echo time used. A gradient-echo sequence was used with a flip angle of 35°, a matrix of 128 × 256 pixels, a phase encode group size of 8, a field of view of 35cm, and a sampling bandwidth of 250 kHz per pixel. A gating delay of 0ms was employed and the repeat time was adjusted to the patient's heart rate. Each image was acquired during an 8 to 13 second breath-hold, depending on the patient's heart rate and thoracic girth. A full-thickness region of interest was then used to calculate the $T2^*$ value (see appendix 1).

The liver $T2^*$ value was determined as follows: A single 10 mm slice through the center of the liver was scanned at a series of eight different echo times (2.2–20.1 ms). Each image was acquired during a 10 to 13 second breath-hold (varying with abdominal girth). A gradient-echo sequence was used with a repeat time of 200 ms, a flip angle of 20°, a matrix of 96 × 128 pixels, a field of view of 35 cm and a sampling bandwidth of 125 kHz per pixel. An area of interest in the liver parenchyma was then used in the same way as that in the myocardium to calculate the $T2^*$ value.

Patients were then scanned at 1.5 Tesla, with a Siemens Sonata scanner (Siemens Medical Solutions, Erlangen, Germany.) The gradient echo sequence parameters were the same as those outlined for the Picker scanner, with the following differences. For the liver acquisitions eight slightly different echo times (2.3–20.0 ms) were used, and the sampling bandwidth was 488 kHz per pixel. For the heart acquisitions nine slightly different echo times (5.6–18.0 ms) were used, and the repetition time between two radio-frequency pulses was between 7.4 and 18.6 ms, depending on the echo time used. 9 segments were used, and the sampling bandwidth was 488kHz per pixel. Analysis was as detailed above using a Siemens analysis package. After 20 minutes the scan was repeated in 13 patients who had been removed from the Siemens scanner in the interim period to assess interstudy reproducibility.

Results: There was a significant, linear correlation between $T2^*$ values obtained for both the heart and the liver between scanners. The mean heart $T2^*$ value obtained was 14.2 ms and 14.5 ms for the Siemens and the Picker scanners respectively, with a mean difference of 0.4 ms and variability of 1.3 ms. The coefficient of variability between scanners was 8.8%. The mean heart $T2^*$ values obtained for interstudy assessment were 14.2 ms for the first assessment, and then 13.6 ms for the repeat assessment, with a mean difference of 0.6 ms and a variability of 0.7 ms. The coefficient of variability for reproducibility was 3.9%.

For the liver, the mean liver $T2^*$ value obtained was 6.21 ms on the Siemens and 7.11 ms on the Picker scanner, with a mean difference of 0.90 ms and a variability of 1.4 ms. The coefficient of variability was 8.5% between scanners. The mean liver $T2^*$ values obtained for interstudy assessment were 3.9 ms for the first assessment, and then 4.0 ms for the repeat assessment, with

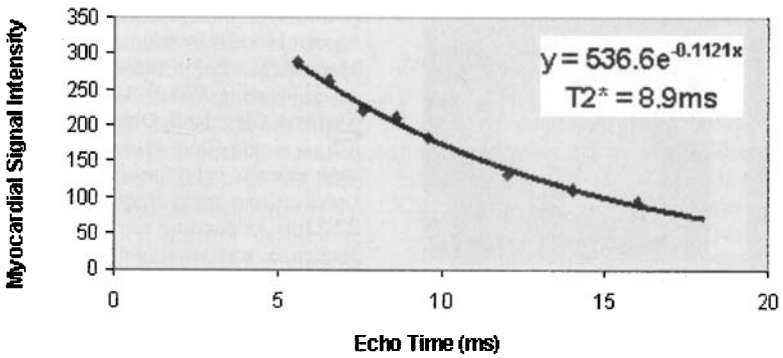

Figure 2. A series of midventricular short axis slices through the myocardium are shown, along with the varying echo times for each image. The signal intensity of an area of interest in the interventricular septum (including both the epicardial and endocardial regions) is then measured, and then subtracted from the background intensity of the image. These net values are then plotted against the echo time as seen below, and fit to an exponential decay curve y=ke-TE/T2*, where k is a constant, and TE represents the echo time.

a mean difference of 0.1 ms and a variability of 0.2 ms. The coefficient of variability for reproducibility was 3.3%.

Conclusion: This is a straightforward, robust technique which allows the non-invasive measurement of tissue iron deposition, and is transferable and reproducible. The use of breath-hold, gradient-echo acquisitions allows reliable quantification of myocardial and liver iron.

318. Comparing Velocity-Encoded MRI with Doppler Ultrasound in the Velocity–Time Integral Method of Analyzing the Aortic Valve in Patients with Aortic Stenosis

Shelton D. Caruthers,[1] Shiow Jiuan Lin,[1] Mary Watkins,[1] Peggy Brown,[1] Katherine Lehr,[1] Latish Mckinney,[1] Gregory Lanza,[1] Samuel Wickline.[1] [1]*Cardiovascular MR Labs & Philips Medical Systems, 660 S. Euclid – Campus Box 8086, St. Louis, MO, USA*

Introduction: The analysis of heart valves can be easily and accurately performed using Doppler ultrasound. While quantifying flow with MRI using velocity-encoding techniques is becoming more widely accepted, the in vivo validation of MRI in quantifying flow through the valves has scant support in the literature. Receiving even less attention are MRI-based applications of the continuity equation based on the conservation of mass. With ultrasound, the velocity–time integrals (VTI) are measured before and after the valve; and, with a measure of left ventricular outflow tract (LVOT) diameter, the aperture of the aortic valve can be calculated. We propose to perform similar calculations with velocity-encoded MRI.

Purpose: The purpose of this study is to define the reliability of velocity-encoded MRI as a routine method for quantifying the area of stenotic aortic valves in patients. Furthermore, the purpose is to compare this method with the accepted standard of Doppler ultrasound for characterization of valvular dysfunction. Specifically, the VTI acquired proximal and distal to valves using both Doppler ultrasound and MRI are compared for calculation of absolute valve dimension by the continuity equation. MR and ultrasound measurements of pressure gradients across the aortic valve are also compared.

Methods: Fourteen patients with aortic valve stenosis were imaged using a 1.5T whole body MRI (Philips Medical Systems, Best, Netherlands). In addition to standard cine views for qualitative assessment of function, multiple velocity-encoded cine MR images were acquired (TE/TR/a = 2.9/6/30, FoV = 350 mm, Matrix 128 × 256, thk = 9 mm, 30 frames/heartbeat). The maximum encoding velocity parameter was chosen such that no flow aliasing occurred in the systolic flow jet (typically about 4 m/s in the aorta, 3 m/s in the LVOT). Two imaging planes parallel to the aortic valve plane were interrogated—one placed in the ascending aorta 1.5cm distal to the aortic valve plane, and one in the LVOT at 1.5cm proximal to the valve plane (see Fig. 1). Quantitative flow data was analyzed on an offline workstation (EasyVision R5.1, Philips Medical Systems). To calculate VTI, the area under the curve of the peak flow velocity versus time was summed over systole. VTI was calculated at each level and statistically compared to the respective Doppler ultrasound measurements of Aortic VTI and LVOT VTI. Using the modified Bernoulli equation (4 times velocity squared), peak and mean gradients were also calculated and compared by the two methods. Using the Pearson correlation test, similarity of ultrasound and MRI values were tested for each of these parameters.

Results: The VTI measurements between velocity-encoded MRI and Doppler ultrasound correlated well. Correlation coefficients between ultrasound and MRI measurements of VTI were $r = 0.94$ for Aorta and $r = 0.90$ for LVOT ($p < 0.001$) (see fig. 2). Similarly, using these values in the continuity equation to calculate valve size gave a correlation coefficient between methods of $r = 0.85$ ($p < 0.001$). Using this VTI method, the average valve size for these 14 patients was $1.1 \pm 0.4\,cm^2$ for ultrasound and $1.1 \pm 0.3\,cm^2$ for MRI, showing no difference between methods in a paired t-test (see fig. 3). Calculations of the pressure gradients, both mean and peak, also correlated well ($r = 0.91$ and 0.92, respectively). The average peak pressure gradient for these patients was 23.1 ± 10.8

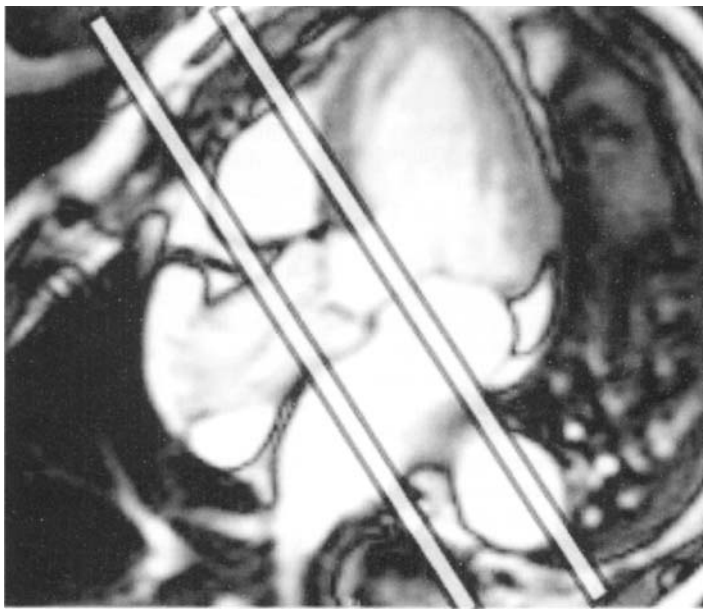

Figure 1. Example positioning of the 2 imaging slices parallel to stenotic aortic valve for acquiring velocity-encoded images.

mmHg measured with MRI compared with 29.5 ± 15.5 mmHg for ultrasound.

Conclusion: Velocity-encoded MRI can be used as a reliable tool to evaluate flow through stenotic aortic valves. The measurements of pressure gradients, VTI, and the valve diameter as calculated by the VTI continuity equation method all correlate well with the accepted standard of Doppler ultrasound.

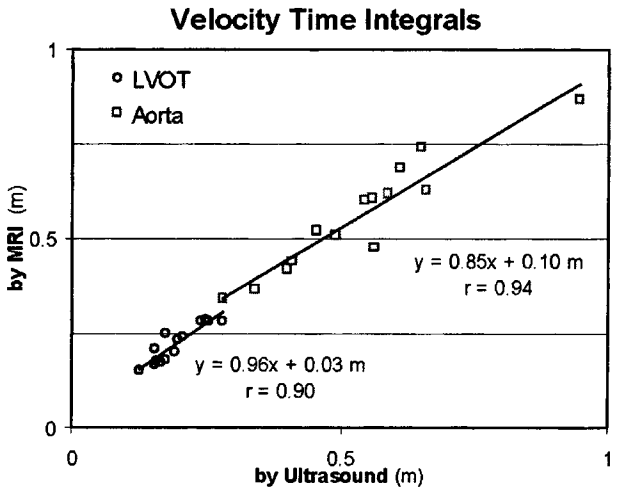

Figure 2. Velocity–Time Integrals for both Aorta and LVOT agree well between velocity-encoded MRI and Ultrasound methods.

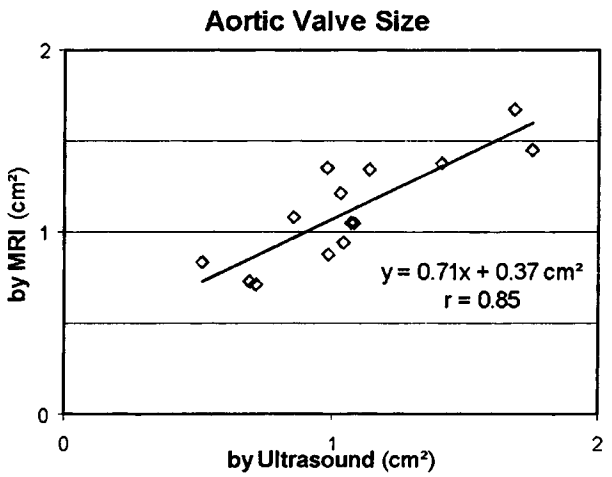

Figure 3. Calculating functional aortic valve area by the continuity equation gives the same result using Ultrasound or velocity-encoded MRI.

319. Interstudy Reproducibility of Right Ventricular Measurements with Cardiovascular Magnetic Resonance in a Mixed Study Population. Comparison with Left Ventricular Results

Frank Grothues,[1] Gillian Smith,[2] Nick Bellenger,[2] James Moon,[2] Helmut Klein,[1] Dudley Pennell.[2] [1]*University of Magdeburg, Leipziger Strasse 44, Magdeburg, Germany;* [2]*Royal Brompton and Harefield NHS Trust, Sydney Street, London, United Kingdom*

Introduction: Fast breath-hold Cardiovascular Magnetic Resonance (CMR) is considered the gold standard in assessing left ventricular (LV) volumes, ejection fraction (EF) and mass. Excellent results for interstudy reproducibility have been reported by our group that are superior to results achieved with Echocardiography (SCMR 2001). Interstudy reproducibility of right ventricular parameters has not been investigated so far. Despite the fact, that there is usually paid less attention to the right ventricle, measurement of RV function can be equally important in the assessment of the severity of mitral/aortic regurgitation and the course of pulmonary hypertension or congenital heart disease with left to right shunting (e.g. atrial septal defect).

Purpose: CMR with its inherent advantage of a true three-dimensional data acquisition is an excellent method for the assessment of the complex RV architecture, which can only be insufficiently described by geometric models. We investigated 60 subjects in total (20 normal volunteers, 20 patients with congestive heart failure (CHF) of ischemic or dilated cardiomyopathy origin, and 20 patients with left ventricular hypertrophy [LVH]) for comparison of interstudy reproducibility of RV parameters with according LV measurements.

Methods: All 60 subjects (47 male, mean age 51 ± 18 yrs) underwent two CMR studies with a short interval between each study. A stack of contiguous cine gradient echo short axis cines was acquired and end-diastolic/end-systolic epicardial and endocardial borders both in RV and LV were traced for calculation of mass, end-diastolic volume (EDV) and end-systolic volume (ESV), from which stroke volume (SV) and EF could be derived.

Results: The interstudy variability (mean difference between measurements) and percentage variability of the

Table 1

Interstudy Variability ± SD

		Normals	CHF	LVH	Total
EDV	LV	2.2 ± 4.3ml	−2.3 ± 7.6ml	0.4 ± 7.3ml	0.1 ± 6.7ml
	RV	1.1 ± 6.5ml	0.4 ± 10.9ml	3.7 ± 8.5ml	1.7 ± 8.8ml
ESV	LV	1.5 ± 2.8ml	−1.6 ± 7.4ml	−0.7 ± 4.6ml	−0.3 ± 5.3ml
	RV	−0.3 ± 4.7ml	1.2 ± 10.6ml	2.0 ± 9.6ml	1.0 ± 8.6ml
SV	LV	0.9 ± 4.0ml	−1.0 ± 5.9ml	1.2 ± 5.5ml	0.4 ± 5.2ml
	RV	1.3 ± 5.4ml	−0.8 ± 5.0ml	1.3 ± 9.5ml	0.6 ± 6.7ml
EF	LV	−0.5 ± 1.7%	0.1 ± 2.4%	0.7 ± 2.2%	0.1 ± 2.1%
	RV	0.6 ± 2.7%	−0.8 ± 5.4%	0.0 ± 6.2%	−0.1 ± 4.9%
Mass	LV	−1.1 ± 4.2g	0.7 ± 9.6g	−2.4 ± 8.4g	−1.0 ± 7.7g
	RV	−0.4 ± 4.7g	0.7 ± 6.0g	−1.4 ± 5.8g	−0.4 ± 5.5g

Table 2

% Variability ±SD

		Normals	CHF	LVH	Total
EDV	LV	2.8 ± 1.9	3.0 ± 1.9	3.8 ± 2.4	3.2 ± 2.1
	RV	3.5 ± 2.1	5.8 ± 5.2	5.6 ± 4.5	5.0 ± 4.2**
ESV	LV	6.3 ± 4.9	4.1 ± 4.0	7.7 ± 5.3	6.0 ± 4.9
	RV	7.6 ± 7.5	12.1 ± 17.4	13.8 ± 11.5	11.1 ± 12.8**
SV	LV	3.2 ± 2.3	7.1 ± 4.1	4.4 ± 3.6	4.9 ± 3.7
	RV	4.7 ± 2.6	6.5 ± 4.0	7.9 ± 8.7	6.4 ± 5.8
EF	LV	2.2 ± 1.0	6.0 ± 4.5	3.0 ± 1.7	3.7 ± 3.2
	RV	3.4 ± 2.3	6.2 ± 6.6	7.0 ± 7.9	5.5 ± 6.2*
Mass	LV	2.3 ± 1.7	3.8 ± 2.7	2.8 ± 2.4	3.0 ± 2.3
	RV	6.2 ± 3.7	7.1 ± 5.0	8.5 ± 5.3	7.3 ± 4.7***

measured parameters for LV and RV for each subgroup are shown in Tables 1 and 2 below. No within subgroup differences were detected. Looking at the total study population, with the exception of stroke volume the interstudy percentage variability was significantly higher in RV measurements compared to the correspondent LV values (*$p < 0.05$, **$p < 0.01$, ***$p < 0.001$). However, interstudy percentage variability for the RV showed good results ranging from 5% (for EDV) to 11% (for ESV) in the total study group.

Conclusion: In a direct comparison, CMR showed good interstudy reproducibility of RV parameters in study population of normals, heart failure and hypertrophy. Although reproducibility was lower compared to left ventricular values, CMR is a reliable method and can be considered a gold standard for serial assessment of RV volumes, function and mass.

320. Does the Adage, "There Is Safety in Numbers" Lead Us Astray? An MRI Remodeling Study

Robert Biederman,[1] Martin Aldrich,[1] Walter Rogers,[1] Sunil Mankad,[1] Jane Ripple,[1] June Yamrozik,[1] Kathleen Simpson,[1] James Magovern,[1] Nathaniel Reichek.[2] [1]*Allegheny General Hospital, 320 East North Avenue, Pittsburgh, PA USA;* [2]*St. Francis Hospital, Rosalyn, NY USA*

Introduction: A review of English manuscripts for the past two decades regarding LV mass regression and/or LV remodeling in aortic stenosis (AS) patients undergoing echocardiography pre and post aortic valve replacement (AVR) disclosed 18 articles. The mean number of patients required to detect a significant improvement was 230 ± 102 (12–1103) with a mean duration of 19 ± 18mo(1–60mo).

Purpose: Since cardiac MR (CMR) provides true 3D data with high spatial resolution and resultant increases in accuracy with decreased variability of measurement, we tested the hypothesis that CMR could detect significant regression in LV mass and improvement in indices of LV remodeling in a smaller series of routine patients with a short study duration.

Methods: Six patients with severe AS underwent CMR (GE:CV/i) at baseline and 5.5 ± 0.5 months after AVR. LVmass, LVEDV, LVESV and EF using Simpson's rule were measured, along with 1D circumferential segmental shortening (%S), in 5 patients.

Results: LVmass (g) and LVmass index (g/m2) were significantly decreased after AVR: LVM PRE = 177 ± 77 vs POST = 150 ± 62g, ($p < 0.01$) and LVMI PRE = 95 ± 22 vs POST = 81 ± 23g/m2), ($p < 0.002$). LVmass/vol (g/m2/ml) was also significantly improved post AVR: PRE = 0.85 ± 0.23 vs POST = 0.69 ± 0.12, ($p < 0.05$) indicating potentially favorable reverse remodeling in these 6 pts. While EF was similar at baseline and remained unchanged post AVR (68 ± 14 vs 65 ± 12, p = NS), mean%S improved after AVR (23 ± 12 to 25 ± 12, $p < 0.05$). Further, it could be shown that in just the 3 patients without CAD %S was significantly improved (26 ± 12 vs 28 ± 10, $p = 0.05$). No change in %S could be demonstrated for the 2 patients with CAD (18 ± 10 vs 19 ± 13, p = NS). Regarding transmural function, at all levels (endocardial, midwall, and epicardial) %S was markedly depressed in the CAD group (n = 2) compared to no CAD (n = 3) patients ($p < 0.05$) preoperatively. After AVR, while both groups demonstrated augmentation of intramyocardial strain, the CAD group transmural strain remained significantly less than the non CAD group, ($p < 0.01$ for all). Similarly, evidence of significant LVMI regression could be demonstrated for both the CAD (n = 4) and non CAD group (n = 2), ($p \leq 0.05$) while a fall in LVMI/vol ratio could be demonstrated only in CAD patients who had higher PRE values (0.81 ± 0.07 vs 0.69 ± 08 ($g/m^2/ml$), $p < 0.05$).

Conclusion: CMR's high fidelity imaging of LV structure and chamber, as well as intramyocardial function, permit estimations of remodeling with an order of magnitude fewer patient requirements than echocardiography, facilitating more efficient and timely observations of important biologic phenomena.

321. Does the Type of Prosthesis Influence Early Left Ventricular Mass Regression Following Aortic Valve Replacement? Assessment with Magnetic Resonance Imaging (MRI)

Penelope Sensky,[1] Mahmoud Loubani,[1] Richard Keal,[1] Nilesh Samani,[1] Andrew Sosnowski,[1] Manuel Galinanes.[1] [1]*Glenfield Hospital, Groby Road, Leicester, Leicestershire, United Kingdom*

Introduction: In patients with aortic stenosis, persisting left ventricular (LV) hypertrophy is an independent outcome measure following aortic valve replacement (AVR). Debate exists regarding selection of the best valve prosthesis to enhance early LV mass regression. It has been suggested that stentless valves are haemodynamically superior to their stented counterparts and may lead to more rapid regression of LV hypertrophy. Similarly, the more laminar flow created by mechanical bileaflet valves compared with the tilting disc design has also been proposed to enhance LV remodelling. Previous studies evaluating LV mass regression following AVR with varying prosthesis types have used echocardiography to measure LV mass. These studies are frequently underpowered and conflicting results are presented in the literature.

Purpose: To compare the degree of LV mass regression measured by MRI, six months after prospectively randomized valve implantation for two biological prostheses, i.e. stented and stentless, and for two mechanical valves, i.e. tilting disc and bileaflet.

Methods: Forty consecutive patients (age 63 ± 11 years, 23 male, 17 female) with pure aortic stenosis accepted for elective AVR were included. 20 patients requiring tissue prosthesis were prospectively randomized to receive either Freestyle stentless or Mosaic stented (Medtronic Inc., Minneapolis, USA) valves. The other 20 patients requiring mechanical prosthesis were randomized to have either Aortech tilting disc (Aortech Europe Limited, Scotland, UK) or ATS bileaflet prostheses. LV mass measurements were performed with magnetic resonance imaging (1.5 Tesla Vision, Siemens, Germany) immediately prior to (A) and six months after (B) surgery. Sequential contiguous short axis slices covering the heart from base to apex were acquired with the use of a breath-hold cine gradient echo sequence (TR = 60 ms, TE = 4.8 ms, FOV = 420 × 315mm, slice thickness = 6mm, 96 × 128

Table 1

Mean ± SD Valve Size (mm) Implanted, LV Mass Index (g) at Visits A and B, LV Mass Index Change (δ), Pre and Post Operative Maximum Valve Gradients

	Mosaic	Freestyle	Aortech	ATS
Valve size	24.6 ± 1.58	24.6 ± 4.3	24.7 ± 1.86	23.8 ± 1.69
LVMI A	118.8 ± 26.4	98.3 ± 33.5	111 ± 33.4	98.2 ± 23.2
LVMI B	88.6 ± 18.5	74.1 ± 15.9	87 ± 17.9	71.9 ± 18.5
δ LVMI	24.1 ± 11.1	21.1 ± 16.7	19.3 ± 9.5	26.3 ± 10.8
p Values; A vs. B	$p < 0.001$	$p < 0.01$	$p < 0.01$	$p < 0.001$
Pre-op max gradient	88.7 ± 20.5	925.8 ± 21.7	88.9 ± 21.3	79.2 ± 17.7
Post-op max gradient	25.7 ± 10.7	14.9 ± 6.6	27 ± 14.3	20.6 ± 9.8

matrix, acquisition over 15, 19 or 23 heart beats). Images were transferred to a computer workstation (Sun Microsystems, Mountain View, California) for analysis with dedicated software (Argus II, Siemens, Erlangen, Germany). Epicardial and endocardial borders of each slice were contoured by hand on diastolic and systolic imaging frames to allow calculation of LV mass (slice summation method). Specific myocardial density of $1.05 g\,cm^{-3}$ was used. Echocardiography was used to establish haemodynamic prosthesis performance. The study was powered to a 10 g change in LV mass with power of 90% and $p < 0.05$ [1].

Results: Thirtynine patients completed the study. Echocardiographic severity of aortic stenosis and post-operative haemodynamic measurements were similar in all valve groups. Significant LV mass regression occurred in all patients. The degree of early mass regression was similar with all prostheses studied (table 1).

Conclusion: MRI is the current reference standard for measurement of chamber size and volumes and this is reflected in its reproducibility. Use of MRI has demonstrated that the extent of early left ventricular mass regression following aortic valve replacement in patients with pure aortic stenosis is not influenced by the type of valve prosthesis implanted. Further longitudinal clinical trials with the use of MRI techniques to accurately evaluate haemodynamic and left ventricular parameters are needed to confirm the benefits of the stentless prostheses and to establish the effects of differing mechanical valves on ventricular remodeling with time.

322. Left Ventricular Systolic Dysfunction and Impaired Aortic Compliance Among Moderate-Term Survivors of Hodgkin's Mantle Radiation: A CMR Study

Ming Hui Chen,[1] Peter Danias,[2] Ethan Cash,[3] Elizabeth Cameron,[3] Carol Salton,[2] Kraig Kissinger,[2] Rebecca Gelman,[3] Jay Harris,[1] Peter Mauch,[1] Warren Manning.[2] [1]*Brigham and Women's Hospital, Cardiovascular Division, Boston, Massachusetts, United States;* [2]*Beth Israel Deaconess Medical Center, 330 Brookline Ave, Boston, Massachusetts, United States;* [3]*Dana-Farber Cancer Institute, Boston, Massachusetts United States*

Introduction: Mantle radiation (XRT) treatment for Hodgkin's disease includes a large portion of the heart and aorta in the radiation portals. While XRT may lead to late (>10 year) clinical cardiovascular disease as evidenced by premature coronary artery disease and pericardial constriction, the presence of subclinical left ventricular systolic dysfunction or aortic disease in asymptomatic moderate-term survivors is unknown. Cardiovascular magnetic resonance imaging (CMR) is uniquely suited to evaluate subclinical cardiovascular disease.

Purpose: The purpose of this study was to use CMR to determine whether patients treated >5 years previously with mantle XRT have subclinical left ventricular dysfunction and aortic disease.

Methods: We studied 13 subjects (39 ± 10yrs; 5 men) with history of Hodgkin's disease who had received XRT >5 yrs prior to enrollment. No subject had received chemotherapy. None had clinical symptoms of cardiovascular disease. CMR was performed to assess resting left ventricular systolic function (N = 12) and abdominal aortic elasticity (N = 7). For functional cardiac imaging we used a Philips 1.5T ACS NT scanner with an ECG-triggered fast field echo (FFE) sequence with an echoplanar (EPI) readout (300–360 mm FOV), slice thickness 10 mm, matrix 128 × 256, TE = 9.1 msec). Subjects were imaged supine on a flat table in an anatomic position replicating that of XRT treatment. Left ventricular function was defined as abnormal if the global ejection fraction was <5th percentile of a community-based population cohort (men <59%; women <60%). Aortic elasticity data were compared to a control group of healthy adult men (29 ± 5 yrs).

Results: Twelve subjects were included in the analysis. One subject with claustrophobia did not complete the protocol. Left ventricular dysfunction was common in those with history of Hodgkin's disease and previous XRT, with 6 of 12 subjects (50%) having depressed global left ventricular ejection fraction ($p = 0.0001$, range 51–58%). HD subjects also had significantly decreased abdominal aortic elasticity as compared with controls, with decreased vessel compliance (0.14 ± 0.06 vs. 0.20 ± 0.05 mm2/kPa/mm, p=0.01), increased pressure–strain elastic modulus (75 ± 36 vs. 51 ± 16 kPa, p=0.02) and increased stiffness index (7.0 ± 2.6 vs. 4.9 ± 1.2, p=0.004). Of note, systolic blood pressure between subjects and controls

were not significantly different (BP 121 ± 19/50 vs. 115 ± 6/50, $p > 0.05$).

Conclusion: In this study of Hodgkin's disease subjects treated > 5 years previously with mantle XRT, we found CMR evidence of subclinical left ventricular systolic dysfunction and impaired abdominal elasticity. The clinical implications and possible progression to overt disease remain to be defined.

323. Evaluation of Aortic Stenosis by Direct Planimetric Assessment of the Aortic Valve Area Using Steady-State Free Precession Sequences (Balanced FFE)

Torsten Sommer,[1] Matthias Hackenbroch,[1] Ralf Kader,[1] Ulrich Hofer,[1] Heyder Omran,[1] H. Schild.[1] [1]*University of Bonn, Sigmund-Freud-Strasse 25, Bonn, NRW, Germany*

Introduction: In magnetic resonance (MR) imaging the severity of aortic stenosis is commonly evaluated by measuring the maximum transvalvular flow and calculating the pressure gradients. This method alone is known to be inaccurate, especially in patients with concomitant aortic regurgitation and impaired left ventricular function. Therefore a technique for direct measurement of the aortic valve opening area is of high clinical interest. Recently developped steady-state free precession sequences (balanced fast field echo [b-FFE]) allow precise identification of cardiac valves, wildely independent of turbulent transvalvular flow and valvular calcifications.

Purpose: The aim of this study was to evaluate b-FFE sequences in the planimetric assessment of aortic valve area in patients with suspected aortic valve stenosis in comparison with multiplane transesophageal echocardiography (TEE).

Methods: 32 patients with suspected aortic stenosis underwent MR imaging (Intera, 1.5 T, Philips Medical Systems) and TEE (System 5, GE) with a 6.7 MHz multiplane probe for evaluation of the aortic valve. B-FFE sequences (TE 1.39, TR 2.8 ms, flip angle 70°, voxel size 2mm × 2mm × 6 mm, 30 heart phases) were acquired during breathhold in an imaging plane perpendicular to the aortic annulus to identify the cross sectional aortic valve area. Planimetric measurements of the aortic valve opening area in early systole were performed by MRI and TEE. Planimetry was performed manually, and three repeated measurements were averaged for MRI and TEE. The mean values of all orifice areas were compared with the t-test for paired data. The correlation between two variables was evaluated by linear regression analysis.

Results: Image quality was adequate for evaluation in all MRI and TEE studies. Acquisition time for MRI was 25 ± 6 min (mean ± standard deviation), evaluation time for planimetry was <5 min in all cases. There was an excellent correlation between MR and TEE-derived measurements of aortic valve area (correlation coefficient $r = 0.93$). MR measured a mean aortic valve area of 1.39 ± 0.79 (SD) cm^2 compared with 1.24 ± 0.71 cm^2 derived from multiplane TEE. The mean difference between the 2 methods was 0.11 ± 0.2 cm^2.

Conclusion: Exact determination of the orifice area of a stenotic aortic valve is essential to guide therapy. Using standard methods, such as cardiac catheterization, Doppler-flow or MR-flow studies, the orifice area has to be calculated by empirically-derived formulas, which may be susceptible to changes in hemodynamic status, leading to an inter-study variability of the orifice area in aortic stenosis of up to 20%. Direct measurement of the orifice area is possible by transesophageal echocardiography, but may be limited by valvular calcifications due to strong reflection of the ultrasound signal and distal signal loss. Conventional gradient echo sequences (such as FFE or FLASH) may also be hampered by artifacts due to calcifications and/or turbulent flow. Balanced FFE sequences represent a new method, which is characterized by the fact that the time integrated area (over one TR, between two Radio frequency excitation pulses) of each gradient waveform is zero. Susceptibility artifacts due to calcifications are reduced. Blood produces a very bright signal, independent of flow and motion, and shows an excellent contrast with soft tissues such as myocardium or cardiac valves.

To our knowledge, this is the first MRI study using steady-state free precession sequences for the determination of valve area in patients with aortic stenosis. The method proved to be robust, easy to apply and highly accurate in the determination of stenotic valve area. B-FFE sequences allow evaluation of stenotic aortic valves by direct planimetric assessment of the valve area with excellent correlation to multiplane TEE.

324. The Relationships Between MRI-Determined Left Ventricular Mass and Body Composition Variables

Saul Myerson,[1] Keith George,[2] Karen Birch,[2] Michael World,[3] Dudley Pennell.[4] [1]*Royal Brompton Hospital, Sydney Street, London, UK;* [2]*Manchester Metropolitan University, Alsager Campus, Alsager, Cheshire, UK;* [3]*Royal Defence Medical College, Gosport, Portsmouth, Hampshire, UK;* [4]*Royal Brompton and Harefield NHS Trust, Sydney Street, London, United Kingdom*

Introduction: The relationships between left ventricular mass (LVM) and body composition variables have been examined previously in order to scale LVM to body size. The best index for LVM is debated however and although lean mass has been suggested, its measurement is difficult. Data collection has occurred primarily via echocardiography and anthropometry although the inaccuracies of these techniques hamper studies in this area.

Purpose: We sought to examine the relationship between LVM and a range of body composition variables (lean body mass; fat mass; visceral fat mass; sub-cutaneous fat mass) and other anthropometrically determined body size parameters (height; weight; body surface area) using the highly accurate techniques of cardiac and whole body magnetic resonance imaging.

Methods: Data was collected in 172 young, healthy, adult male subjects (age range 17–28). The association with LVM was examined by allometric scaling analysis to determine the linearity of each relationship, and thus the ability to use a simple ratio for the scaling of LVM. Initial linearity checks suggested that most of the relationships between LVM and the body composition and size variables were non-linear, thus precluding the simple ratio approach to scaling. Log–log least squares linear regression analyses were performed for each

body size and composition variable to determine the slope exponent (b) of the relationship with LVM.

Results: Geometric consistency was confirmed for LVM-lean body mass($b = 0.90 \pm 0.15$) and LVM-BSA ($b = 1.30 \pm 0.24$). However, only lean body mass had a linear relationship with LVM and is suitable for simple ratio scaling. LVM-weight ($b = 0.80 \pm 0.13$) and LVM-height ($b = 1.41 \pm 0.60$) did not include the geometrically consistent values of 1.0 and 3.0 within their respective confidence intervals. Exponents for all indices of adiposity were generally very low suggesting only a small positive relationship (e.g. LVM-FM $b = 0.20 \pm 0.06$).

Conclusion: This study supports the use of lean mass as a valid index for simple ratio scaling of LV mass. For other parameters, simple ratio scaling should be avoided in attempting to produce body-size-independent cardiac indices as the relationships are non-linear.

325. Myocardial Involvement in Systemic Lupus Erythematodes — Visualization by Contrast Enhanced Cardiac MRI

Jeanette Schulz-Menger,[1] Natalie Siegle,[2] Alexander Natusch,[3] Erika Gromnica-Ihle,[3] Rainer Dietz,[4] Matthias Friedrich.[2]
[1]*Franz-Volhard-Klinik, Wiltbergstrasse 50, Berlin, Germany;* [2]*Franz-Volhard-Klinik, Charite, Wiltbergstr. 50, Berlin, Germany;* [3]*Rheuma-Klinik, Klinikum Buch, Karower Chaussee 30, Berlin, Germany;* [4]*Franz-Volhard-Klinik, Charite Campus Buch, Wiltbergstr. 50, Berlin, Germany*

Introduction: Systemic lupus erythematodes (sLE) is a systemic rheumatic disease involving different organs. Cardiac manifestation is more commonly found at autopsy than clinically detected. Similary, the incidence of myocarditis in autopsy studies is about 40%, whereas it is clinically found in up to 10% of patients.

Contrast enhanced magnetic resonance imaging was shown to be suitable to detect myocardial injury due to different causes.

Purpose: The purpose of this study was to assess myocardial function and contrast enhancing properties of patients with acute sLE as compared to stable sLE and healthy volunteers.

Methods: We performed contrast-enhanced MRI in 18 patients with proven sLE. 10 patients suffered from a stable disease (sLE), whereas 8 patients suffered from acute disease as defined by the ECLAM activity score and ANA antibody titers (sLE acute). We applied standard T1-weighted multislice spin-echo sequences (TE 30ms; TR 480–725 ms; slice thickness 6 mm) in axial and short axis views before and after application of 0.1 mmol/kg Gd-DTPA (Magnevist®, Schering AG; Berlin, Germany) on conventional MRI systems (1.0 T; Siemens-Expert; Siemens AG, Erlangen, Germany and 1.5 TSigna CV/i; GE; Milwaukee, USA, respectively) using the body coil. The relative global signal enhancement (RE) of the myocardium as related to that of the skeletal muscle was calculated. Furthermore, we compared the left ventricular ejection fraction (LVEF) as determined by gradient echo sequences. Results of both patient groups were compared with 10 healthy volunteers (vol).

Results: The RE of patients with acute sLE (5.5 ± 0.9) was significantly higher than that of the other patients with sLE (3.0 ± 0.4; $p < 0.004$). The RE of the volunteers (2.0 ± 0.3) was significant lower as compared to that of acute sLE ($p < 0.0001$), whereas there was no significant difference to the group of stable sLE-patients.

There were no significant difference of the LVEF between any of the groups (vol $70 \pm 2\%$; sLE $69 \pm 4\%$; sLE acute $68 \pm 3\%$; p = n.s.).

The contrast enhancement was markedly subendocardial in all patients with acute disease, in contrast to 50% of the other sLE patients and none of the volunteers.

Conclusion: Patients with acute sLE reveal a normal LVEF, but evidence for acute myocardial injury as detected by ceMRI. The cause of the observed more subendocardial distribution of the contrast enhancement is unclear, but may be related to small vessel inflammation.

Thus, contrast enhanced MRI may be very helpful in the detection of myocardial involment in patients with systemic lupus erythematodes.